

Quantum critical transport in the unitary Fermi gas

Tilman Enss

Physik Department, Technische Universität München, D-85747 Garching, Germany

The thermodynamic and transport properties of the unitary Fermi gas at finite temperature T are governed by a quantum critical point at $T = 0$ and zero density. We compute the universal shear viscosity to entropy ratio η/s in the high-temperature quantum critical regime $T \gg |\mu|$ and find that this strongly coupled quantum fluid comes close to perfect fluidity $\eta/s = \hbar/(4\pi k_B)$. Using a controlled large- N expansion we show that already at the first non-trivial order the equation of state and the Tan contact density C agree well with the most recent experimental measurements and theoretical Luttinger-Ward and Bold Diagrammatic Monte Carlo calculations.

PACS numbers: 03.75.Ss, 05.30.Fk, 51.20.+d

I. INTRODUCTION

The unitary Fermi gas is a basic many-body problem which describes strongly interacting fermions ranging from ultracold atoms near a Feshbach resonance [1–3] to dilute neutron matter. The properties in the dilute limit are independent of the microscopic details of the interaction potential and share a common universal phase diagram. A quantum critical point (QCP) at zero temperature governs the critical behavior in the whole phase diagram as a function of temperature T , chemical potential μ , detuning from the Feshbach resonance ν , and magnetic field h [4–6]. In the spin balanced case $h = 0$, and at resonance $\nu = 0$ the Fermi gas is unitary and scale invariant. In terms of the thermal length $\lambda_T = \hbar(2\pi/mk_BT)^{1/2}$ the density equation of state $n\lambda_T^3 = f_n(\mu/k_BT)$ is a universal function which has been measured experimentally [7, 8]. The unitary Fermi gas becomes superfluid at a universal $T_c(\mu) \approx 0.4\mu$ [8], see Fig. 1. In this work we focus on the quantum critical regime $T > 0$ above the QCP at $h = 0$, $\nu = 0$ and $\mu = 0$, where $n\lambda_T^3 = f_n(0) \approx 2.9$ is a universal constant. Since the thermal length λ_T is comparable to the mean particle spacing $n^{-1/3}$, quantum and thermal effects are equally important. There is no small parameter, and it is a theoretical challenge to compute the critical properties. Recent measurements [8] and computations [9] of the equation of state now agree to the percent level. However, a precise determination of transport properties is much more demanding.

In order to reliably estimate transport coefficients we perform controlled calculations in a large- N expansion [5, 10]. We obtain new results for the Tan contact density [11–13] and the transport properties in the quantum critical region. The shear viscosity $\eta = \hbar\lambda_T^{-3}f_\eta(\mu/k_BT)$ assumes a universal value at $\mu = 0$. In kinetic theory $\eta = P\tau$ is given by the pressure P times the viscous scattering time τ , which is related to the incoherent relaxation time of the gapless critical excitations above the QCP. The entropy density $s = k_B\lambda_T^{-3}f_s(\mu/k_BT)$ at $\mu = 0$ is exactly proportional to the pressure, $s = 5P/2T$, and the viscosity to entropy ratio (at $N = 1$)

$$\frac{\eta}{s} = \frac{2}{5}T\tau \approx 0.74 \frac{\hbar}{k_B} \quad (1)$$

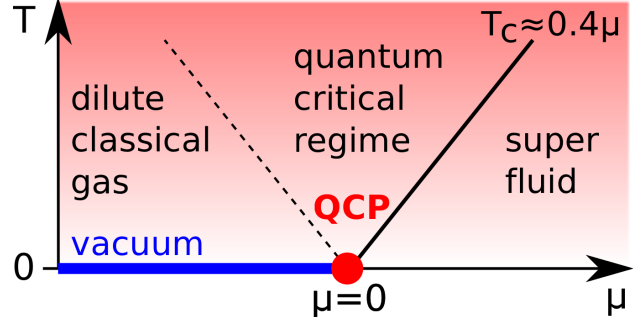


FIG. 1: Universal phase diagram of the unitary Fermi gas.

is a universal number *independent of temperature*. A temperature independent ratio $\eta/s = \hbar/(4\pi k_B)$ has been found in certain string theories [14] and is conjectured to hold as a lower bound in other models [15]. Strongly interacting quantum fluids which saturate this bound are called perfect fluids [16]. Among real non-relativistic fluids the unitary Fermi gas comes closest to the bound and is almost perfect [17–19], while for graphene the viscosity decreases logarithmically with temperature in the quantum critical regime [20].

We compare our large- N results at $N = 1$ [21] with experimental measurements [8, 18, 22, 23] and other theoretical approaches, including self-consistent Luttinger-Ward [17, 24, 25] and Bold Diagrammatic Monte Carlo (BDMC) [9] calculations, see Table I.

	experiment	large- N	LuttWard	BoldDiagMC
$n\lambda_T^3$	2.966(35) [8]	2.674	3.108 [25]	2.90(5) [9]
$P [nk_BT]$	0.891(19) [8]	0.928	0.863 [25]	0.90(2) [9]
$s [nk_B]$	2.227(38) [8]	2.320	2.177 [25]	2.25(5) [9]
$C [k_F^4]$		0.0789	0.084 [17]	0.080(5) [26]
$\eta/s [\hbar/k_B]$	1.0(2) [18, 27]	0.741	0.708 [17]	

TABLE I: Thermodynamic properties and transport coefficients of the unitary Fermi gas in the quantum critical region $\mu = 0$, $T > 0$: density n , pressure P , entropy density s , Tan contact density C , and shear viscosity η , with Fermi momentum $k_F = (3\pi^2 n)^{1/3}$. Large- N results extrapolated to $N = 1$.

The excellent agreement between experiment and BDMC provides a reliable reference to assess the accuracy of other methods. We find very good agreement of the pressure P with large- N (3% above BDMC) and Luttinger-Ward (4% below), just slightly outside the error bars, and similarly good agreement for the entropy density s . From the BDMC equation of state simulations of [9], one can extract (via the pair propagator) a preliminary value for the contact density [26] $C/k_F^4 = 0.080(5)$. Our large- N value is just 1.4% below BDMC, which is remarkable given how simple the calculation is, while Luttinger-Ward lies about 5% above BDMC, just inside the error bars. Experimental measurements of the contact [23] yield $C = 0.030(6) k_F^4$ for the trapped gas at $\mu = 0$ ($T/T_F = 0.64$), which agrees well with trap averaged calculations [23]. However, knowledge of the trap averaged contact does not allow to reconstruct the corresponding value for the homogeneous system, so we refrain from a direct comparison. Dynamical and transport properties such as η/s are harder to compute than thermodynamic properties, which makes simple approximations all the more valuable: we find that η/s agrees to 5% between large- N and Luttinger-Ward theory, giving a narrow estimate. The viscosity of a trapped gas has been measured experimentally and agrees with trap averaged calculations [18, 22, 27], but differs from the viscosity of the homogeneous system.

The body of this paper explains how these values are obtained: in section II we review the RG analysis of the unitary Fermi gas and its universal phase diagram, in section III we perform thermodynamic and transport calculations using the controlled large- N expansion, and in section IV we extract the $\mu = 0$ data from the self-consistent Luttinger-Ward calculation. The results from the different approaches are discussed in section V. In particular, in Appendix A we give a new derivation of the Tan adiabatic and energy relations and show that they are satisfied *exactly* in self-consistent Luttinger-Ward approximations, while Appendix B provides technical details on the quantum kinetic equation.

II. PHASE DIAGRAM OF THE UNITARY FERMION GAS

The interacting two-component Fermi gas is described by the action

$$S_F = \int d^d x d\tau \left\{ \sum_{\sigma} \psi_{\sigma}^* \left(\partial_{\tau} - \frac{\nabla^2}{2m} - \mu_{\sigma} \right) \psi_{\sigma} + g_0 \psi_{\uparrow}^* \psi_{\downarrow}^* \psi_{\downarrow} \psi_{\uparrow} \right\} \quad (2)$$

where ψ_{σ} are Grassmann variables representing fermion species $\sigma = \uparrow, \downarrow$ of equal mass m , and the imaginary time $\tau = 0 \dots \beta$ runs up to the inverse temperature $\beta = 1/T$ (we use units where $\hbar = 1 = k_B$). μ_{σ} is the chemical potential of species σ , but we will only consider the spin-balanced case $\mu = \mu_{\uparrow} = \mu_{\downarrow}$.

In $d = 3$ dimensions the scattering amplitude for small relative momenta k can be written in the form [2]

$$f(k) = \frac{1}{-1/a - ik + r_e k^2/2} \quad (3)$$

where the scattering length a can be varied experimentally by an applied magnetic field, and the effective range r_e depends on the details of the interatomic potential. By fine-tuning to a Feshbach resonance $1/a \rightarrow 0$ the two-particle scattering remains strong at low energy $k \rightarrow 0$ and reaches the unitarity limit $f(k) = i/k$ independent of r_e . The low-energy properties remain universal at finite density $n > 0$ if r_e is much shorter than the mean particle spacing $n^{-1/3}$. This condition $k_F r_e \rightarrow 0$ is realized physically for a dilute gas and near a broad Feshbach resonance as in ^6Li [2].

A finite r_e regularizes the contact interaction at short distances (UV), and for a sharp momentum cutoff $\Lambda \sim 1/|r_e|$ the detuning ν is related to the bare coupling g_0 in (2) by

$$\nu \equiv -\frac{1}{a} = -\frac{4\pi}{m} \left(\frac{1}{g_0} + \frac{m\Lambda}{2\pi^2} \right). \quad (4)$$

Note that the resonance $\nu = 0$ can only be reached for attractive interactions $g_0 < 0$, when a bound state of the interatomic potential is at the continuum threshold.

More generally, this can be understood from an RG analysis of the model (2): at zero temperature and density the running coupling g obeys the *exact* flow equation [4–6]

$$\frac{dg}{d\ell} = (2-d)g - \frac{g^2}{2} \quad (5)$$

which in $2 < d < 4$ has an unstable fixed point at $g_* = -2(d-2) < 0$ corresponding to the Feshbach resonance. For smaller $g < g_*$ the fermions will form a BEC of fermion pairs; for larger $g > g_*$ the flow runs toward the attractive fixed point $g = 0$ of the free Fermi gas (BCS limit). At the Feshbach resonance fixed point the detuning ν is a relevant perturbation with scaling dimension $\dim[\nu] = d - 2$.

The zero temperature phase diagram exhibits a quantum critical point at the Feshbach resonance $\nu = 0$, zero chemical potential $\mu = 0$, and zero spin imbalance $h = 0$, where the “magnetic field” h couples to the difference in chemical potential $\mu_{\uparrow} - \mu_{\downarrow}$. This critical point determines a universal phase diagram for finite T , ν , μ and h [5, 6]. In this work we concentrate on the spin balanced gas $h = 0$ at unitarity $\nu = 0$: the phase diagram for finite T and μ is depicted in Fig. 1.

On the lower right for $\mu/T > (\mu/T)_c$ there is a superfluid phase of fermion pairs, while the left part is a normal Fermi liquid phase at finite density. The phase transition line $T_c(\mu) \approx 0.4\mu$ [8] is universal and strictly linear, in contrast to the corresponding phase diagram for a dilute Bose gas [4]. On the left for $\mu/T \rightarrow -\infty$ the Fermi liquid crosses over to a dilute classical gas. The

line $T = 0$, $\mu < 0$ has zero density (vacuum). Here we focus on the high-temperature quantum critical regime $T \gg |\mu|$, and in the following we compute the thermodynamic and transport properties specifically for the representative value $\mu = 0$.

It is useful to perform a Hubbard-Stratonovich transformation to decouple the fermion interaction. We introduce a complex field $\phi(x, \tau)$ representing a fermion pair and write the Bose-Fermi action

$$S_{BF} = \int d^d x d\tau \left\{ \sum_{\sigma} \psi_{\sigma}^* \left(\partial_{\tau} - \frac{\nabla^2}{2m} - \mu_{\sigma} \right) \psi_{\sigma} - \frac{1}{g_0} |\phi|^2 - \phi \psi_{\uparrow}^* \psi_{\downarrow}^* - \phi^* \psi_{\downarrow} \psi_{\uparrow} \right\}. \quad (6)$$

Note that the pairing field ϕ has a positive gap because $g_0 < 0$ near the Feshbach resonance. The action (6) has the same critical behavior as the two-channel atom-molecule model at its zero-range fixed point [2, 5].

One can now proceed by integrating out the fermions to obtain an effective bosonic action for the pairing field ϕ . This action has bosonic vertices with any even number $2n$ of fields which are given by a bare fermion loop with $2n$ vertex insertions. In contrast to the repulsive Fermi gas, where these vertices are irrelevant in the RG sense, for the unitary Fermi gas these vertices all have marginal scaling. Already the particle-particle loop ($n = 1$), which contributes to the self-energy of the ϕ field, changes the bare scaling dimension $\dim[\phi] = d/2$ of the ϕ field by an anomalous contribution $\eta_{\phi} = 4 - d$ to the true scaling dimension $\dim[\phi] = (d + \eta_{\phi})/2 = 2$, which is independent of d (for $2 < d < 4$). Similarly, all higher bosonic vertices $n > 1$ are singular for small external frequencies and momenta and scale marginally in the RG sense. There is no small parameter to suppress these higher loop diagrams, and they are *a priori* equally important in the infrared (IR). At zero density the $2n > 2$ particle β functions are decoupled from the $2n = 2$ particle β function in Eq. (5), which is therefore exact. Nevertheless, there may also be a three-particle resonance (Efimov effect) in the three-particle β function depending on the mass ratio and whether the particles are fermions or bosons [28]. This changes the ground state from a two-particle to a three-particle bound state and leads to limit cycles in the RG flow [29].

At finite density all higher bosonic vertices couple back into the self-energy of the ϕ field. In order to assess the quantitative importance of these higher vertices, one can introduce an artificial expansion parameter such as the dimension $\epsilon = 4 - d$ for $2 < d < 4$ [30] or $1/N$ for a large number of fermion flavors N [5, 10]. Alternatively, one can use a Monte Carlo sampling of diagrams [9]. In this work we perform a large- N expansion and compare it with the results from other approaches.

III. LARGE-N EXPANSION

We modify the Bose-Fermi action (6) by introducing N identical copies, or flavors, of \uparrow and \downarrow fermions, denoted by $\psi_{\sigma a}$ with $\sigma = \uparrow, \downarrow$ and the flavor index $a = 1, \dots, N$. The pairing field ϕ is chosen to create an $\uparrow\downarrow$ pair of any flavor, and we obtain the action [6, 10]

$$S_{BF} = \int d^d x d\tau \left\{ \sum_{\sigma a} \psi_{\sigma a}^* \left(\partial_{\tau} - \frac{\nabla^2}{2m} - \mu_{\sigma} \right) \psi_{\sigma a} - \frac{N}{g_0} |\phi|^2 - \phi \sum_a \psi_{\uparrow a}^* \psi_{\downarrow a}^* - \phi^* \sum_a \psi_{\downarrow a} \psi_{\uparrow a} \right\}. \quad (7)$$

This action is $O(N)$ invariant under rotations in flavor space. The Gaussian integral over the fermion field yields the effective bosonic action

$$\begin{aligned} S_B &= N \int d^d x d\tau \left\{ -\text{tr}_{\sigma} \ln \begin{bmatrix} \partial_{\tau} - \frac{\nabla^2}{2m} - \mu_{\uparrow} & -\phi \\ -\phi^* & \partial_{\tau} + \frac{\nabla^2}{2m} + \mu_{\downarrow} \end{bmatrix} - \frac{1}{g_0} |\phi|^2 \right\} \\ &= NT \sum_{\omega_m} \sum_{\mathbf{k}} \left\{ \sum_{\sigma} \ln G_{0\sigma}(k, \omega_m) - \mathcal{T}^{-1}(k, \omega_m) |\phi(k, \omega_m)|^2 + \mathcal{O}(|\phi|^4) \right\} \end{aligned} \quad (8)$$

with the trace running over the spin index σ . The bare Fermi propagator $G_{0\sigma}(k, \omega_m)$ is given by

$$G_{0\sigma}^{-1}(k, \omega_m) = -i\omega_m + \varepsilon_k - \mu_{\sigma} \quad (9)$$

with dispersion $\varepsilon_k = k^2/(2m)$, and the bosonic propagator $-\mathcal{T}(k, \omega_m)$ is given by the regularized T -matrix in medium,

$$\begin{aligned} \mathcal{T}^{-1}(k, \omega_m) &= \frac{1}{g_0} + T \sum_{\epsilon_n} \int \frac{d^d p}{(2\pi)^d} G_{0\uparrow}(p, \epsilon_n) \\ &\quad \times G_{0\downarrow}(\mathbf{k} - \mathbf{p}, \omega_m - \epsilon_n). \end{aligned} \quad (10)$$

The number of flavors N appears only as a global prefactor in the action (8), hence a controlled loop expansion is possible [5]. Each closed fermion loop contributes a factor of N , while each ϕ propagator is suppressed by $1/N$. Even though the higher bosonic vertices still have marginal scaling, their contributions to the grand potential are now suppressed quantitatively by powers of $1/N$. For $T \gg \mu$ the system is in the normal phase, and the action (8) has a saddle point at $\langle \phi \rangle = 0$. To order $\mathcal{O}(1/N)$ the grand potential reads

$$\frac{\Omega}{N} = T \sum_{\omega_m} \sum_{\mathbf{k}} \left\{ 2 \ln G_0(k, \omega_m) - \frac{1}{N} \ln \mathcal{T}(k, \omega_m) \right\} \quad (11)$$

Note that this order of the $1/N$ expansion extrapolated to $N = 1$ is exactly the Nozières-Schmitt-Rink (NSR)

theory [21]. The Matsubara frequency summation can be continued analytically to real frequency,

$$\frac{\Omega}{N} = \sum_k \left\{ -2T \ln[1 + e^{-\beta(\varepsilon_k - \mu)}] - \frac{1}{N} \int_{-\infty}^{\infty} \frac{d\omega}{\pi} b(\omega) \delta(k, \omega, \mu, \nu) \right\} \quad (12)$$

with the scattering phase shift $\delta(k, \omega, \mu, \nu) = \text{Im} \ln \mathcal{T}(k, \omega, \mu, \nu)$ and the Bose function $b(\omega) = (\exp(\beta\omega) - 1)^{-1}$. Specifically in $d = 3$ the T -matrix reads (in the spin-balanced case $h = 0$)

$$\begin{aligned} \mathcal{T}^{-1}(k, \omega) = & -\frac{m\nu}{4\pi} - \frac{m^{3/2}}{4\pi} \sqrt{\frac{\varepsilon_k}{2} - \omega - i0 - 2\mu} \\ & + \frac{m}{2\pi^2 k} \int_0^\infty dp \frac{p}{1 + e^{\beta(\varepsilon_p - \mu)}} \\ & \times \ln \left[\frac{\omega + i0 + 2\mu - \varepsilon_p - \varepsilon_{k-p}}{\omega + i0 + 2\mu - \varepsilon_p - \varepsilon_{k+p}} \right]. \quad (13) \end{aligned}$$

The integral is convergent and readily evaluated numerically.

A. Thermodynamics

Using (13) we obtain for the pressure $P = -\Omega/L^d$ (equation of state) at $\mu = 0$, $\nu = 0$, $h = 0$ and $T > 0$:

$$\begin{aligned} \frac{P}{N} = & -\frac{\Omega}{NL^d} = P^{(0)} + \frac{1}{N} P^{(1)} + \dots \\ = & \left(1.734\,400 + \frac{1}{N} 0.747\,561 \right) T \lambda_T^{-3} \quad (14) \end{aligned}$$

where

$$\begin{aligned} P^{(0)} = & 2(1 - 2^{-3/2}) \zeta(5/2) T \lambda_T^{-3} \\ P^{(1)} = & \int \frac{d^3 k}{(2\pi)^3} \frac{d\omega}{\pi} b(\omega) \delta(k, \omega). \end{aligned}$$

Since the unitary Fermi gas is scale invariant the internal energy density ε is proportional to the pressure [31]

$$\frac{\varepsilon}{N} = \frac{3P}{2N} = \left(2.601\,600 + \frac{1}{N} 1.121\,341 \right) T \lambda_T^{-3}. \quad (15)$$

Also the entropy density $s = \partial P / \partial T = (\varepsilon + P - \mu n) / T$ at unitarity and $\mu = 0$ is proportional to the pressure,

$$\frac{s}{N} = \frac{5P}{2TN} = \left(4.335\,999 + \frac{1}{N} 1.868\,902 \right) \lambda_T^{-3}. \quad (16)$$

The density at $\mu = 0$ to order $\mathcal{O}(1/N)$ is

$$\begin{aligned} \frac{n}{N} = & \frac{d(P/N)}{d\mu} = n^{(0)} + \frac{1}{N} n^{(1)} + \dots \\ = & \left(1.530\,294 + \frac{1}{N} 1.143\,936 \right) \lambda_T^{-3} \quad (17) \end{aligned}$$

where

$$\begin{aligned} n^{(0)} = & 2(1 - 2^{-1/2}) \zeta(3/2) \lambda_T^{-3} \\ n^{(1)} = & \int \frac{d^3 k}{(2\pi)^3} \frac{d\omega}{\pi} b(\omega) \frac{d\delta(k, \omega)}{d\mu}. \end{aligned}$$

If this order of the $1/N$ expansion is evaluated at $N = 1$ (NSR) we obtain for the density

$$n = 2.674\,230 \lambda_T^{-3} \quad (N = 1). \quad (18)$$

The ratio of thermal length to mean particle spacing, $\lambda_T n^{1/3} \approx 1.388$, is of order unity, hence quantum and thermal fluctuations are equally important in the high-temperature quantum critical region. The density determines the Fermi temperature

$$k_B T_F = \frac{k_F^2}{2m} = \frac{(3\pi^2 n)^{2/3}}{2m} \quad (19)$$

which is useful to compare with data given in terms of the reduced temperature

$$\theta \equiv \frac{T}{T_F} = \left(\frac{3\sqrt{\pi}}{8} n \lambda_T^3 \right)^{-2/3} = 0.681\,496 \quad (N = 1). \quad (20)$$

Finally, the Tan contact density is defined as the total spectral weight (density) of the pairing field [11–13]

$$\begin{aligned} C = & m^2 \langle \phi^* \phi \rangle = -\frac{m^2}{N} \int \frac{d^3 k}{(2\pi)^3} \frac{d\omega}{\pi} b(\omega) \text{Im} \mathcal{T}(k, \omega) \\ = & 26.840\,128 \frac{\lambda_T^{-4}}{N}. \quad (21) \end{aligned}$$

At $N = 1$ the contact can be expressed in terms of k_F using Eq. (19) and agrees with the BDMC calculation within 1.4% (see Table I), but it differs from the result in [6] by a factor of two.

Note that the Tan adiabatic theorem [12]

$$\frac{d(-P/N)}{d\nu} = \frac{C}{4\pi m} \quad (22)$$

is fulfilled exactly in the $1/N$ expansion: the change of the pressure with detuning is

$$\begin{aligned} \frac{d(-P/N)}{d\nu} = & -\frac{1}{N} \int \frac{d^3 k}{(2\pi)^3} \frac{d\omega}{\pi} b(\omega) \frac{d\delta(k, \omega)}{d\nu} \\ = & -\frac{m}{4\pi N} \int \frac{d^3 k}{(2\pi)^3} \frac{d\omega}{\pi} b(\omega) \text{Im} \mathcal{T}(k, \omega) \quad (23) \end{aligned}$$

because the change of scattering phase shift with detuning is $d\delta(k, \omega)/d\nu = (m/4\pi) \text{Im} \mathcal{T}(k, \omega)$, and using Eq. (21) we obtain (22).

B. Transport

At $N = \infty$ the fermions are free: once a shear flow is excited in the infinite system it will continue forever, and the dynamic shear viscosity is

$$\eta(\omega) = \pi P \delta(\omega). \quad (24)$$

The Drude weight is proportional to the pressure, in accordance with the viscosity sum rule [17, 32] (we obtain twice the value quoted in Ref. [33]). At order $1/N$ the fermions acquire a self-energy correction by scattering off pairing fluctuations, so for large N the fermions are almost free quasi-particles with lifetime $\mathcal{O}(N)$ and an energy shift of the quasi-particle dispersion $\text{Re } \Sigma \sim 1/N$. In kinetic theory the dynamic viscosity becomes

$$\eta(\omega) = \frac{P\tau}{1 + (\omega\tau)^2} \quad (25)$$

with the viscous scattering time $\tau = \mathcal{O}(N)$: the $\delta(\omega)$ function in (24) is broadened to a peak of width $1/N$ and height N . Note that the high-frequency tail $\eta \sim C/15\pi\sqrt{m\omega}$ [17] is not seen in kinetic theory [33].

In order to compute transport properties for large N it is justified to use the quantum Boltzmann equation [4, 34]:

- the fermions propagate as free particles between collisions, up to subleading corrections;
- the collision integral $\text{Im } \Sigma \sim 1/N$ contains only particle-particle scattering described by the medium T -matrix $\mathcal{T}(k, \omega)$ (10), because particle-hole scattering appears at higher orders;
- in addition to the collision (dynamic) term there is the shift of the dispersion (kinetic) term $\text{Re } \Sigma \sim 1/N$ of the same order. However, it is only a subleading correction to the leading real term $\Pi_{xy}/N \sim N^0$ (see below) and can be neglected.

Based on these considerations we arrive at the Boltzmann equation [34, 35]

$$\frac{\partial f}{\partial t} + \dot{\mathbf{r}} \cdot \frac{\partial f}{\partial \mathbf{r}} + \dot{\mathbf{p}} \cdot \frac{\partial f}{\partial \mathbf{p}} = -\frac{1}{N} I[f] \quad (26)$$

for the distribution function $f(\mathbf{p}, \mathbf{r}, t)$, where $I[f]$ is the collision integral. For the shear viscosity we consider a velocity field $\mathbf{u} = u_x(y)\hat{\mathbf{x}}$ with a small shear gradient $\partial u_x/\partial y$, and the local equilibrium distribution $f(\mathbf{p}) = f^0(\epsilon - \mathbf{u} \cdot \mathbf{p})$ with $\epsilon = p^2/2m$. In the stationary limit the Boltzmann equation (26) becomes [35]

$$-\frac{\partial u_x}{\partial y} v_y p_x \frac{\partial f^0}{\partial \epsilon} = -\frac{1}{N} I[f]. \quad (27)$$

The velocity gradient induces a momentum current density

$$\Pi_{xy} = 2N \int \frac{d^3 p}{(2\pi)^3} v_y p_x f(\mathbf{p}) = -\eta \frac{\partial u_x}{\partial y} \quad (28)$$

proportional to $\partial u_x/\partial y$, with the coefficient given by the shear viscosity η . We choose a deviation from the equilibrium distribution, $f = f^0 + \delta f$ with $\delta f = f^0(1 - f^0)\varphi(\mathbf{p})$

and $\varphi(\mathbf{p}) = v_y p_x/T$, such that the momentum current density is

$$\Pi_{xy} = \frac{2N}{T} \int \frac{d^3 p}{(2\pi)^3} v_y^2 p_x^2 f_p^0 (1 - f_p^0) = P. \quad (29)$$

This is equal to the pressure for free fermions ($N = \infty$) at arbitrary temperature, as can be seen by integrating by parts. We can now replace $-\partial u_x/\partial y = P/\eta$ in (27) and take moments of the Boltzmann equation by integrating both sides with $2N \int d^3 p/(2\pi)^3 v_y p_x$. The left-hand side becomes

$$\frac{2NP}{\eta T} \int \frac{d^3 p}{(2\pi)^3} v_y^2 p_x^2 f_p^0 (1 - f_p^0) = \frac{P^2}{\eta} \quad (30)$$

while the right-hand side yields the collision integral [33, 35, 36]

$$\begin{aligned} C_{xy} &= 2 \int \frac{d^3 p}{(2\pi)^3} v_y p_x I[\delta f] \\ &= \frac{2}{T} \int \frac{d^3 p}{(2\pi)^3} v_y p_x \int \frac{d^3 p_1}{(2\pi)^3} \int d\Omega \frac{d\sigma}{d\Omega} |\mathbf{v} - \mathbf{v}_1| \\ &\quad \times f_p^0 f_{p_1}^0 (1 - f_{p'}^0)(1 - f_{p'_1}^0) \\ &\quad \times [\varphi(\mathbf{p}) + \varphi(\mathbf{p}_1) - \varphi(\mathbf{p}') - \varphi(\mathbf{p}'_1)] \end{aligned} \quad (31)$$

where fermions with incoming momenta \mathbf{p}, \mathbf{p}_1 scatter into outgoing momenta $\mathbf{p}', \mathbf{p}'_1$. It will be convenient to express these momenta in terms of the total momentum $\mathbf{q} = \mathbf{p} + \mathbf{p}_1$ and the relative momenta $\mathbf{k} = (\mathbf{p} - \mathbf{p}_1)/2$ ($\mathbf{k}' = (\mathbf{p}' - \mathbf{p}'_1)/2$) of the incoming (outgoing) particles, with $|\mathbf{k}'| = |\mathbf{k}|$ by energy conservation. The occupation numbers give the probability that the incoming states are occupied, and the outgoing states are not. The differential cross section is given by the medium T -matrix

$$\frac{d\sigma}{d\Omega} = \left| \frac{m}{4\pi} \mathcal{T}(\mathbf{p} + \mathbf{p}_1, \omega = \epsilon_p + \epsilon_{p'} - 2\mu) \right|^2. \quad (32)$$

In the vacuum limit the center-of-mass scattering depends only on the relative momentum k ,

$$\frac{d\sigma}{d\Omega} = \frac{a^2}{1 + a^2 k^2} \quad (\text{vacuum}) \quad (33)$$

but at finite density there is an additional dependence on the total momentum q in the medium T -matrix $\mathcal{T}(q, k) = \mathcal{T}(q, \omega = 2\epsilon_{q/2} + 2\epsilon_k - 2\mu)$. In relative coordinates the shear term in Eq. (31) is [37]

$$\varphi(\mathbf{p}) + \varphi(\mathbf{p}_1) - \varphi(\mathbf{p}') - \varphi(\mathbf{p}'_1) = \frac{k_x k_y - k'_x k'_y}{mT/2}. \quad (34)$$

The collision integral then reads

$$\begin{aligned} C_{xy} &= \frac{2}{\pi m T} \int \frac{d^3 q}{(2\pi)^3} \int \frac{d^3 k}{(2\pi)^3} k k_x k_y |\mathcal{T}(q, k)|^2 f_{\mathbf{q}/2+\mathbf{k}}^0 f_{\mathbf{q}/2-\mathbf{k}}^0 \\ &\quad \times \int \frac{d\Omega_{k'}}{4\pi} (k_x k_y - k'_x k'_y) (1 - f_{\mathbf{q}/2+\mathbf{k}'}^0) (1 - f_{\mathbf{q}/2-\mathbf{k}'}^0) \\ &= \frac{1}{30\pi^5 m T} \int dq q^2 \int dk k^7 |\mathcal{T}(q, k)|^2 \\ &\quad \times [I_{\ell=0}^2(q, k) - I_{\ell=2}^2(q, k)] \end{aligned} \quad (35)$$

with the ℓ -wave angular average $I_\ell(q, k)$ over the Fermi distribution functions derived analytically in appendix B (the d -wave average $I_{\ell=2}^2(q, k)$ contributes only 0.2% to the integral (35)). Finally, only two integrals over the radial momenta q and k have to be performed. In the dilute classical regime the collision integral can be computed analytically,

$$C_{xy}^{\text{cl}} = \frac{32\sqrt{2}z^2T^2\lambda_T^{-3}}{15\pi} \quad (36)$$

with fugacity $z = \exp(\beta\mu)$, and in the same limit the pressure is $P_{\text{cl}} = 2zT\lambda_T^{-3}N$. The viscosity is then given by [35]

$$\eta_{\text{cl}} = \frac{P_{\text{cl}}^2}{C_{xy}^{\text{cl}}} = \frac{15\pi\lambda_T^{-3}N^2}{8\sqrt{2}} = 4.165\,203\,\lambda_T^{-3}N^2. \quad (37)$$

In the high-temperature quantum critical regime $T > 0$, $\mu = 0$ the collision integral has to be computed with the full medium T -matrix $\mathcal{T}(q, \omega)$ from Eq. (10), which is done numerically and yields

$$C_{xy} = 0.935\,683\,T^2\lambda_T^{-3} \quad (38)$$

and together with the pressure at leading order in $1/N$, $P = NP^{(0)} = 1.734\,400\,T\lambda_T^{-3}N$, we obtain in the quantum critical regime

$$\eta = \frac{P^2}{C_{xy}} = 3.214\,917\,\lambda_T^{-3}N^2. \quad (39)$$

This value is about 20% lower than in the dilute classical limit (37), which is mostly due to the reduced pressure, while the effects of reduced density and increased medium scattering almost cancel each other in C_{xy} . With the viscous relaxation time $\tau = P/C_{xy}$ and the entropy density $s = 5P/(2T)$ we obtain the universal viscosity to entropy ratio independent of temperature,

$$\frac{\eta}{s} = \frac{2}{5}T\tau = 0.741\,448\,\frac{\hbar N}{k_B}. \quad (40)$$

A related computation of the viscosity using the medium T -matrix has been performed for large attractive interaction $k_F a = -11.8$ which found $\eta = 2.3\hbar n$ for $\mu = 0$ at $T/T_F = 0.7$ [36], slightly larger than our value (39) at $N = 1$. Note that we have evaluated η using only a single moment of the Boltzmann equation (27), but it has been shown that corrections to η from higher moments are less than 2% [38]. A similar transport calculation using the medium T -matrix in two dimensions has been performed recently [39].

IV. LUTTINGER-WARD THEORY

The Luttinger-Ward theory provides a systematic way to obtain self-consistent and conserving approximations, such that the Green functions satisfy all symmetries and

conservation laws of the model [40, 41]. The Luttinger-Ward functional $\Phi[G_\sigma, G_B]$ can be defined in terms of full fermionic propagators G_σ and full bosonic propagators $G_B = -\mathcal{T}$. The exact theory is given by an infinite set of irreducible contributions to the Φ functional which cannot be evaluated in practice, so typically one chooses a subclass of diagrams. For the unitary Fermi gas a very successful approximation is to use ladder diagrams with full fermionic Green functions [24, 25]. Then the full T -matrix is given by an expression similar to (10) but with full Green functions,

$$\mathcal{T}^{-1}(k, \omega_m) = \frac{1}{g_0} + T \sum_{\epsilon_n} \int \frac{d^3p}{(2\pi)^3} G_\uparrow(\mathbf{p}, \epsilon_n) \times G_\downarrow(\mathbf{k} - \mathbf{p}, \omega_m - \epsilon_n). \quad (41)$$

Since we are interested in the high-temperature critical region we consider only the expressions valid in the normal phase. The Luttinger-Ward theory then prescribes that the \uparrow fermionic self-energy is given by scattering a \downarrow fermion off pair fluctuations described by the full T -matrix,

$$\Sigma_\uparrow(k, \omega_m) = T \sum_{\epsilon_n} \int \frac{d^3p}{(2\pi)^3} G_\downarrow(\mathbf{p}, \epsilon_n) \mathcal{T}(\mathbf{k} + \mathbf{p}, \omega_m + \epsilon_n) \quad (42)$$

and analogously for Σ_\downarrow . The Dyson equation determines the full fermionic Green functions

$$G_\sigma^{-1}(k, \omega_m) = -i\omega_m + \varepsilon_k - \mu_\sigma - \Sigma_\sigma(k, \omega_m). \quad (43)$$

This set of equations (41)–(43) is solved self-consistently by iteration [24, 25]. The resulting Green functions in Matsubara frequency can be continued analytically to obtain the spectral functions in real frequency, which show substantial broadening near T_c and additional excitations beyond a single quasi-particle peak [42].

The pressure $P = -\Omega/L^d$ is obtained from the grand potential [25]

$$\Omega = T \sum_{\omega_m} \sum_{\mathbf{k}} \left\{ \sum_{\sigma} \ln G_\sigma(k, \omega_m) + \sum_{\sigma} [1 - G_{0\sigma}^{-1}(k, \omega_m) G_\sigma(k, \omega_m)] - \ln \mathcal{T}(k, \omega_m) \right\} \quad (44)$$

evaluated using the self-consistent fermion propagator and the full T -matrix. We extract the high-temperature quantum critical behavior from the existing thermodynamic data [25] interpolated at $\mu = 0$. Specifically, we make a cubic spline interpolation of $\mu(T)$ and find the solution of $\mu(T) = 0$ at $\theta = T/T_F = 0.6165$, which implies $n\lambda_T^3 = 8/(3\sqrt{\pi})\theta^{-3/2} = 3.108$. Furthermore, we find $P = 0.8630\,nk_B T$, $s = 2.177\,nk_B$, and $C = 0.084\,353\,k_F^4$, which can be recast in terms of λ_T . These values are summarized in Table I and are remarkably close to the experimental values.

The shear viscosity $\eta(T, \omega)$ has been computed in Luttinger-Ward theory as a function of temperature and frequency [17]: it has a Lorentzian peak at low frequency, followed by a universal tail $\eta(T, \omega) \sim C(T)/15\pi\sqrt{m\omega}$ proportional to the contact density. We make a cubic spline interpolation of $\mu(\eta) = 0$ and find the root at $\eta(T, \omega = 0) = 1.5409\hbar n$, which yields $\eta/s = 0.7077\hbar/k_B$. This result is slightly lower than the large- N value in Eq. (40). We note that in this self-consistent calculation the minimum of $\eta/s \approx 0.6\hbar/k_B$ is found at a somewhat lower temperature $T/T_F \approx 0.4$ [17].

V. DISCUSSION

The unitary Fermi gas in the high-temperature quantum critical region is a challenging many-body problem. It is strongly interacting, with the density almost twice the non-interacting value at $\mu = 0$ [8], and has no small expansion parameter. Still, our large- N results at the first non-trivial order beyond the free Fermi gas are already remarkably close to reliable experimental and theoretical results [8, 9]. A main result of the present paper is that this is true also for the transport properties η/s once medium effects are included in the quantum kinetic equation. A possible reason for this good agreement is that large- N and Luttinger-Ward approximations satisfy the Tan adiabatic and energy relations exactly, as we show in Appendix A. In addition, Luttinger-Ward theory exactly fulfills the scale invariance of the unitary Fermi gas [17]. For a better comparison between calculations for the homogeneous system and experiments it would be desirable to have local measurements in the spirit of Ref. [8] also for the contact and transport properties, since the comparison of trap averaged quantities is less sensitive to the details of the temperature dependence.

Acknowledgments

I wish to thank Lars Fritz, Subir Sachdev, Jörg Schmalian, Richard Schmidt, and Wilhelm Zwerger for fruitful discussions and Mark Ku, Thomas Schäfer, Chris Vale, Félix Werner, and Martin Zwierlein for sharing their data.

Appendix A: Exact Tan relations in Luttinger-Ward theory

Consider the fermionic action (2): a small variation of the quadratic term, δG_0^{-1} , will lead to a change in the grand potential

$$\delta\Omega = -\text{tr}(G\delta G_0^{-1}) \quad (\text{A1})$$

with the trace running over space, time and possibly spin indices. However, this equation is often violated if approximations are made for the full Green function G . A

unique feature of conserving approximations, which are derived from a Luttinger-Ward functional $\Phi[G]$, is that Eq. (A1) holds exactly even for approximate Ω and G [43].

For the strongly interacting Fermi gas it is convenient to start from the Bose-Fermi action (6) and define a Luttinger-Ward functional $\Phi[G_\sigma, G_B]$ in terms of both fermionic and bosonic Green functions [17, 24, 25]. Then a variation of the microscopic parameters $\delta G_{0\sigma}^{-1}$ and/or δG_{0B}^{-1} induces a change of the grand potential [17]

$$\delta\Omega = -\text{tr}(G_\sigma\delta G_{0\sigma}^{-1}) + \text{tr}(G_B\delta G_{0B}^{-1}). \quad (\text{A2})$$

Again, this exact equation continues to hold within conserving approximations with full self-consistent propagators G_σ and G_B .

We will now show that the Tan adiabatic theorem [12]

$$\frac{d\Omega/L^d}{d(-1/a)} = \frac{C}{4\pi m} \quad (\text{A3})$$

and the Tan energy formula [11]

$$\varepsilon = \sum_\sigma \int \frac{d^3k}{(2\pi)^3} \varepsilon_k \left(n_{k\sigma} - \frac{C}{k^4} \right) + \frac{C}{4\pi m a} \quad (\text{A4})$$

are consequences of (A2) and therefore hold not only in the exact theory but in any conserving approximation, including the self-consistent T -matrix approximation introduced in section IV. A variation of detuning changes only the bosonic quadratic term

$$G_{0B}^{-1}(k, \omega_m) = -\frac{1}{g_0} = \frac{m}{4\pi} \left(-\frac{1}{a} + \frac{2\Lambda}{\pi} \right) \quad (\text{A5})$$

in the action (6),

$$\frac{\partial G_{0\sigma}^{-1}(k, \omega_m)}{\partial(-1/a)} = 0 \quad \frac{\partial G_{0B}^{-1}(k, \omega_m)}{\partial(-1/a)} = \frac{m}{4\pi}. \quad (\text{A6})$$

The variation of the grand potential is then

$$\begin{aligned} \frac{d\Omega}{d(-1/a)} &= -\text{tr} \left(G_\sigma \frac{\partial G_{0\sigma}^{-1}}{\partial(-1/a)} \right) + \text{tr} \left(G_B \frac{\partial G_{0B}^{-1}}{\partial(-1/a)} \right) \\ &= \frac{m}{4\pi} \text{tr}(G_B) \end{aligned} \quad (\text{A7})$$

with the density of bosons expressed by the Tan contact density,

$$\begin{aligned} L^{-3} \text{tr}(G_B) &= T \sum_{\omega_m} \int \frac{d^3k}{(2\pi)^3} G_B(k, \omega_m) e^{+i0\omega_m} \\ &= G_B(x=0, \tau=-0) = \langle \phi^* \phi \rangle = \frac{C}{m^2}. \end{aligned} \quad (\text{A8})$$

Inserting (A8) into (A7) directly yields the adiabatic theorem (A3). In order to derive the energy formula we consider a variation of mass,

$$\varepsilon = m^{-1} \frac{d\Omega/L^3}{d(m^{-1})}. \quad (\text{A9})$$

Usually this yields only the kinetic energy (cf. Eq. (61) in [43]), but in our case also the interaction term $4\pi a/m$ depends on mass, so (A9) is the full internal energy $\varepsilon = \langle H \rangle$ including the potential term. Specifically,

$$m^{-1} \frac{\partial G_{0\sigma}^{-1}(k, \omega_m)}{\partial m^{-1}} = \varepsilon_k \quad (\text{A10})$$

$$m^{-1} \frac{\partial G_{0B}^{-1}(k, \omega_m)}{\partial m^{-1}} = \frac{m}{4\pi} \left(\frac{1}{a} - \frac{2\Lambda}{\pi} \right), \quad (\text{A11})$$

and with the momentum distribution function $-T \sum_{\omega_m} G_{\sigma}(k, \omega_m) = n_{k\sigma}$ we obtain the internal energy density

$$\begin{aligned} \varepsilon &= -\frac{m^{-1}}{L^3} \text{tr} \left(G_{\sigma} \frac{\partial G_{0\sigma}^{-1}}{\partial m^{-1}} \right) + \frac{m^{-1}}{L^3} \text{tr} \left(G_B \frac{\partial G_{0B}^{-1}}{\partial m^{-1}} \right) \\ &= \sum_{\sigma} \int^{\Lambda} \frac{d^3 k}{(2\pi)^3} \varepsilon_k n_{k\sigma} + \frac{m}{4\pi} \left(\frac{1}{a} - \frac{2\Lambda}{\pi} \right) \frac{C}{m^2} \end{aligned} \quad (\text{A12})$$

where the k integral extends to the momentum cutoff Λ . The regularization term $\Lambda C/(2\pi^2 m)$ can be written as $\sum_{\sigma} \int d^3 k / (2\pi)^3 \varepsilon_k C/k^4$, and we arrive at the energy formula (A4). In a similar way the Tan pressure relation has been derived in the Luttinger-Ward theory by an infinitesimal scale transformation on the grand potential [17]. This concludes our proof that the Tan relations are fulfilled exactly in the self-consistent T -matrix approximation.

Appendix B: Quantum kinetic equation

A useful feature of $d = 3$ dimensions is that the angular averages of the distribution functions can be performed analytically. One can write the product of Fermi functions in (35) with $|\mathbf{k}'| = |\mathbf{k}|$ as

$$\begin{aligned} &f(\varepsilon_{\mathbf{q}/2+\mathbf{k}})f(\varepsilon_{\mathbf{q}/2-\mathbf{k}})[1-f(\varepsilon_{\mathbf{q}/2+\mathbf{k}'})][1-f(\varepsilon_{\mathbf{q}/2-\mathbf{k}'})] \\ &= \frac{1}{4(\cosh a + \cosh bx)(\cosh a + \cosh bx')} \end{aligned} \quad (\text{B1})$$

with $x = \hat{\mathbf{k}} \cdot \hat{\mathbf{q}}$, $x' = \hat{\mathbf{k}}' \cdot \hat{\mathbf{q}}$ and $a = (\varepsilon_{\mathbf{q}/2} + \varepsilon_{\mathbf{k}} - \mu)/T$, $b = kq/(2mT)$. The angular average over the solid angles of the vectors \mathbf{q} , \mathbf{k} and \mathbf{k}' is then

$$\begin{aligned} &\int \frac{d\Omega_{\mathbf{q}}}{4\pi} \int \frac{d\Omega_{\mathbf{k}}}{4\pi} \int \frac{d\Omega_{\mathbf{k}'}}{4\pi} k_x k_y (k_x k_y - k'_x k'_y) f f [1-f] [1-f] \\ &= \frac{k^4}{15} \left(I_{\ell=0}^2(q, k) - I_{\ell=2}^2(q, k) \right) \end{aligned} \quad (\text{B2})$$

where we have defined the ℓ -wave angular average of the distribution functions

$$I_{\ell}(q, k) = \frac{1}{4} \int_{-1}^1 dx \frac{P_{\ell}(x)}{\cosh a + \cosh bx} \quad (\text{B3})$$

with Legendre polynomials $P_{\ell}(x)$. The s -wave average is given by

$$I_{\ell=0}(q, k) = \frac{1}{2b \sinh a} \ln \frac{\cosh[(a+b)/2]}{\cosh[(a-b)/2]} \quad (\text{B4})$$

while the d -wave average can be expressed in terms of polylogarithms $\text{Li}_s(z)$,

$$\begin{aligned} I_{\ell=2}(q, k) &= I_{\ell=0}(q, k) - \frac{1}{4b^3 \sinh a} \\ &\times \left[6 \text{Li}_3(-e^{a+b}) - 6 \text{Li}_3(-e^{b-a}) - 6b \text{Li}_2(-e^{a+b}) \right. \\ &\quad \left. + 6b \text{Li}_2(-e^{b-a}) + a(a^2 - 3ab + \pi^2) \right]. \end{aligned} \quad (\text{B5})$$

Thus, all angular integrations can be done analytically and only the two radial integrations over q and k in Eq. (35) need to be performed numerically.

-
- [1] W. Ketterle and M. Zwierlein, *Rivista del Nuovo Cimento* **31**, 247422 (2008).
 - [2] I. Bloch, J. Dalibard, and W. Zwerger, *Rev. Mod. Phys.* **80**, 885 (2008).
 - [3] S. Giorgini, L. P. Pitaevskii, and S. Stringari, *Rev. Mod. Phys.* **80**, 1215 (2008).
 - [4] S. Sachdev, *Quantum Phase Transitions* (Cambridge University Press, 1999).
 - [5] P. Nikolić and S. Sachdev, *Phys. Rev. A* **75**, 033608 (2007).
 - [6] S. Sachdev, in *The BCS-BEC Crossover and the Unitary Fermi Gas*, edited by W. Zwerger (Springer, Berlin, 2012).
 - [7] S. Nascimbène, N. Navon, K. J. Jiang, F. Chevy, and C. Salomon, *Nature* **463**, 1057 (2010).
 - [8] M. J. H. Ku, A. T. Sommer, L. W. Cheuk, and M. W. Zwierlein, *Science* **335**, 563 (2012).
 - [9] K. Van Houcke, F. Werner, E. Kozik, N. Prokof'ev, B. Svistunov, M. J. H. Ku, A. T. Sommer, L. W. Cheuk, A. Schirotzek, and M. W. Zwierlein (2012), preprint arXiv:1110.3747, *Nature Physics* (in press).
 - [10] M. Y. Veillette, D. E. Sheehy, and L. Radzihovsky, *Phys. Rev. A* **75**, 043614 (2007).
 - [11] S. Tan, *Ann. Phys. (N.Y.)* **323**, 2952 (2008).
 - [12] S. Tan, *Ann. Phys. (N.Y.)* **323**, 2971 (2008).
 - [13] E. Braaten, in *The BCS-BEC Crossover and the Unitary Fermi Gas*, edited by W. Zwerger (Springer, Berlin, 2012).

- [14] G. Policastro, D. T. Son, and A. O. Starinets, Phys. Rev. Lett. **87**, 081601 (2001).
- [15] P. K. Kovtun, D. T. Son, and A. O. Starinets, Phys. Rev. Lett. **94**, 111601 (2005).
- [16] T. Schäfer and D. Teaney, Rep. Prog. Phys. **72**, 126001 (2009).
- [17] T. Enss, R. Haussmann, and W. Zwerger, Ann. Phys. (N.Y.) **326**, 770 (2011).
- [18] C. Cao, E. Elliott, J. Joseph, H. Wu, J. Petricka, T. Schäfer, and J. E. Thomas, Science **331**, 58 (2011).
- [19] G. Wlazłowski, P. Magierski, and J. E. Drut (2012), preprint arXiv:1204.0270v1.
- [20] M. Müller, J. Schmalian, and L. Fritz, Phys. Rev. Lett. **103**, 025301 (2009).
- [21] P. Nozières and S. Schmitt-Rink, J. Low Temp. Phys. **59**, 195 (1985).
- [22] C. Cao, E. Elliott, H. Wu, and J. E. Thomas, New J. Phys. **13**, 075007 (2011).
- [23] E. D. Kuhnle, S. Hoinka, P. Dyke, H. Hu, P. Hannaford, and C. J. Vale, Phys. Rev. Lett. **106**, 170402 (2011).
- [24] R. Haussmann, Phys. Rev. B **49**, 12975 (1994).
- [25] R. Haussmann, W. Rantner, S. Cerrito, and W. Zwerger, Phys. Rev. A **75**, 023610 (2007).
- [26] K. Van Houcke, F. Werner, E. Kozik, N. Prokof'ev, and B. Svistunov, private communication.
- [27] T. Schäfer and C. Chafin, in *The BCS-BEC Crossover and the Unitary Fermi Gas*, edited by W. Zwerger (Springer, Berlin, 2012).
- [28] Y. Nishida, D. T. Son, and S. Tan, Phys. Rev. Lett. **100**, 090405 (2008).
- [29] S. Moroz, S. Floerchinger, R. Schmidt, and C. Wetterich, Phys. Rev. A **79**, 042705 (2009).
- [30] Y. Nishida and D. T. Son, Phys. Rev. A **75**, 063617 (2007).
- [31] T. L. Ho, Phys. Rev. Lett. **92**, 090402 (2004).
- [32] E. Taylor and M. Randeria, Phys. Rev. A **81**, 053610 (2010).
- [33] M. Braby, J. Chao, and T. Schäfer, New J. Phys. **13**, 035014 (2011).
- [34] K. Damle and S. Sachdev, Phys. Rev. B **56**, 8714 (1997).
- [35] P. Massignan, G. M. Bruun, and H. Smith, Phys. Rev. A **71**, 033607 (2005).
- [36] G. M. Bruun and H. Smith, Phys. Rev. A **72**, 043605 (2005).
- [37] H. Smith and H. H. Jensen, *Transport Phenomena* (Oxford University Press, 1989).
- [38] G. M. Bruun and H. Smith, Phys. Rev. A **75**, 043612 (2007).
- [39] T. Enss, C. Küppersbusch, and L. Fritz, in preparation.
- [40] J. M. Luttinger and J. Ward, Phys. Rev. **118**, 1417 (1960).
- [41] G. Baym and L. P. Kadanoff, Phys. Rev. **124**, 287 (1961).
- [42] R. Haussmann, M. Punk, and W. Zwerger, Phys. Rev. A **80**, 063612 (2009).
- [43] G. Baym, Phys. Rev. **127**, 1391 (1962).